Magnetostructural Studies on Ferromagnetically Coupled Copper(II) Cubanes of Schiff-Base Ligands

Arindam Mukherjee,[a] Rajamani Raghunathan,[b] Manas K. Saha,[a] Munirathinam Nethaji,[a] Suryanarayanasastry Ramasesha,*[b] and Akhil R. Chakravarty*[a]

Dedicated to Professor F. Albert Cotton on the occasion of his 75th birthday

Abstract: Three cubane copper(II) clusters, namely $[Cu_4(HL')_4]$ (**1**), $[Cu_4L_2(OH)_2]$ (**2**), and $[Cu_4L_2(OMe)_2]$ (**3**), of two pentadentate Schiff-base ligands *N*,*N*′-(2-hydroxypropane-1,3-diyl)bis(acetylacetoneimine) (H_3L') and *N*,*N*′-(2-hydroxypropane-1,3-diyl)-bis(salicylaldimine) (H_3L), are prepared, structurally characterized by X-ray crystallography, and their variable-temperature magnetic properties studied. Complex **1** has a metal-to-ligand stoichiometry of 1:1 and it crystallizes in the cubic space group $P\bar{4}3n$ with a structure that consists of a tetranuclear core with metal centers linked by a μ_3-alkoxo oxygen atom to form a cubic arrangement of the metal and oxygen atoms. Each ligand displays a tridentate binding mode which means that a total of eight pendant binding sites remain per cubane molecule. Complexes $[Cu_4L_2(OH)_2]$ (**2**) and $[Cu_4L_2(OMe)_2]$ (**3**) crystallize in the orthorhombic space group *Pccn* and have a cubane structure that is formed by the self-assembly of two $\{Cu_2L\}^+$ units. The variable-temperature magnetic susceptibility data in the range 300–18 K show ferromagnetic exchange interactions in the complexes. Along with the ferromagnetic exchange pathway, there is also a weak antiferromagnetic exchange between the copper centers. The theoretical fitting of the magnetic data gives the following parameters: $J_1 = 38.5$ and $J_2 = -18\ cm^{-1}$ for **1** with a triplet ($S=1$) ground state and quintet ($S=2$) lowest excited state; $J_1 = 14.7$ and $J_2 = -18.4\ cm^{-1}$ for **2** with a triplet ground state and singlet ($S=0$) lowest excited state; and $J_1 = 33.3$ and $J_2 = -15.6\ cm^{-1}$ for **3** with a triplet ground state and quintet lowest excited state, where J_1 and J_2 are two different exchange pathways in the cubane $\{Cu_4O_4\}$ core. The crystal structures of **2**·6 H_2O and **3**·2 H_2O·THF show the presence of channels containing the lattice solvent molecules.

Keywords: copper complexes · cubane complexes · ferromagnetism · magnetic properties · Schiff bases · self-assembly

Introduction

High-nuclearity, discrete molecular transition-metal complexes are of current interest for their possible utility in modeling the multimetal active sites of metalloproteins,[1–4] in molecular magnetism, with a special emphasis on single-molecule magnets (SMM),[5,6] and for devising nanometer-sized materials for potential use in nanoscience.[7,8] We have been interested in developing the chemistry of high-nuclearity copper(II) complexes due to their magnetostructural properties, which are not only relevant to the active-site properties of multinuclear copper oxidases,[5b,9,10] but also in the field of molecular magnetism. We have successfully synthesized copper(II) complexes of different nuclearities, varying from three to twelve, by using mono- and binuclear

[a] A. Mukherjee, Dr. M. K. Saha, Dr. M. Nethaji, Prof. Dr. A. R. Chakravarty
Department of Inorganic and Physical Chemistry
Indian Institute of Science, Sir C. V. Raman Avenue
Bangalore 560 012 (India)
Fax: (+91) 080-236-01552
E-mail: arc@ipc.iisc.ernet.in

[b] R. Raghunathan, Prof. Dr. S. Ramasesha
Solid State and Structural Chemistry Unit
Indian Institute of Science, Sir C. V. Raman Avenue
Bangalore 560 012 (India)
Fax: (+91) 080-236-00683
E-mail: ramasesh@sscu.iisc.ernet.in

Supporting information for this article (The packing diagrams in color and the variable-temperature magnetic susceptibility data for **1**–**3**) is available on the WWW under http://www.chemeurj.org/ or from the author.

 DOI: 10.1002/chem.200401048

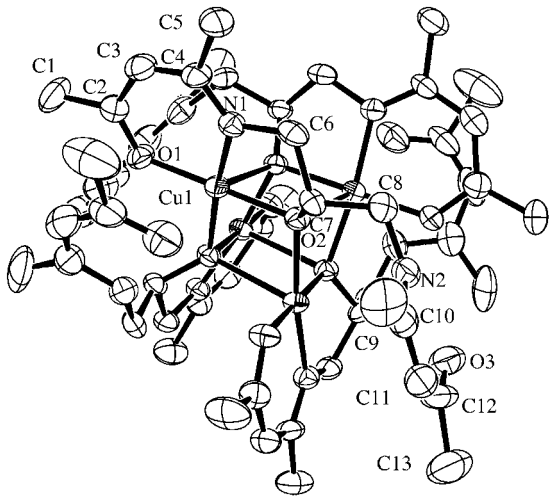

Figure 1. Molecular structure of $[Cu_4(HL')_4]\cdot 4H_2O$ ($\mathbf{1}\cdot 4H_2O$) (ORTEP view; 50% probability thermal ellipsoids).

copper(II) complexes as building blocks by a self-assembly process.[11–15]

The present work stems from our interest in exploring this chemistry further by using the multidentate Schiff-base ligands *N*,*N*′-(2-hydroxypropane-1,3-diyl)bis(salicylaldimine) (H_3L) and *N*,*N*′-(2-hydroxypropane-1,3-diyl)bis(acetylacetoneimine) (H_3L'). Under different reaction conditions we have been able to isolate two different types of copper(II) cubane complexes (see Scheme 1). Copper(II) cubanes are of interest for their magnetic properties, which are tunable by making small variations in the structural parameters.[16–34] Owing to flexibility in the coordination geometry around copper(II) centers, with varied distortions due to a pseudo-Jahn–Teller effect, copper(II) cubanes can show ferro- as well as antiferromagnetic exchange interactions depending on the Cu–O–Cu bridging angles and the planar/pyramidal nature of the bridging oxygen in the Cu_4O_4 core. Among several copper(II) cubanes reported to date, a couple of them only show a magnetic ground state.[16–23] Herein, we report the synthesis, crystal structure, and magnetic properties of three copper(II) cubanes $[Cu_4(HL')_4]\cdot 4H_2O$ ($\mathbf{1}\cdot 4H_2O$), $[Cu_4L_2(OH)_2]\cdot 6H_2O$ ($\mathbf{2}\cdot 6H_2O$), and $[Cu_4L_2(OMe)_2]\cdot 2H_2O\cdot C_4H_8O$ ($\mathbf{3}\cdot 2H_2O\cdot THF$). Their magnetic data were theoretically fitted to obtain the exchange-parameter values and the energy-level diagram for determining the ground state. A preliminary report on the structural aspects of $[Cu_4(HL')_4]\cdot 4H_2O$ ($\mathbf{1}\cdot 4H_2O$) has been published.[23]

Results and Discussion

Synthesis and general aspects: Complexes **1–3** were synthesized in good yields by two different synthetic procedures (Scheme 1). Complex **1** was prepared from the reaction of copper(II) perchlorate hexahydrate with the potentially pentadentate Schiff base *N*,*N*′-(2-hydroxypropane-1,3-diyl)bis(acetylacetoneimine) (H_3L') in CH_2Cl_2/MeOH to form the discrete tetranuclear copper(II) cubane cluster $[Cu^{II}_4(HL')_4]$ (**1**), which has a metal-to-ligand molar ratio of 1:1 [Eq. (1)].

$$4\,[Cu(H_2O)_6](ClO_4)_2 + 4\,H_3L' + 8\,NEt_3 \rightarrow [Cu_4(HL')_4] + 8\,Et_3NHClO_4 + 24\,H_2O \quad (1)$$

$$2\,[Cu_2LBr] + 2\,KOH \rightarrow [Cu_4L_2(OH)_2] + 2\,KBr \quad (2)$$

$$2\,[Cu_2LBr] + 2\,NEt_3 + 2\,MeOH \rightarrow [Cu_4L_2(OMe)_2] + 2\,Et_3NHBr \quad (3)$$

Complexes **2** [Eq. (2)] and **3** [Eq. (3)] were synthesized by using a different synthetic procedure in which the dimeric precursor $[Cu_2LBr]$ self-assembles in the presence of KOH or NEt_3, respectively, in MeOH/EtOH solvent to form the cubane clusters with a metal-to-ligand molar ratio of 2:1. The complexes were characterized from their analytical and spectral data. Complex **1** displays a d–d band at 630 nm in MeOH, whereas in complexes **2** and **3** this band appears at about 640 nm.

Crystal structures: $[Cu_4(HL')_4]$ (**1**) crystallizes in the cubic space group $P\bar{4}3n$ with one copper, one dianionic ligand (HL'), and one lattice water in the crystallographic asymmetric unit (Figure 1). Selected bond lengths and angles for $\mathbf{1}\cdot 4H_2O$ are given in Table 1. The structure consists of a tetranuclear copper(II) core with the metal centers linked by a μ_3-alkoxo-oxygen atom of the Schiff base to give a cubic Cu_4O_4 arrangement of the metal and oxygen atoms. There are six molecules in the unit cell and the 3D packing has vacant space due to the presence of the pendant arm of the ligand, which causes a low density (1.180 g mL^{-1}) of the crystal. The potentially pentadentate ligand (H_3L') binds in a tridentate form through one imine nitrogen, one enolized oxygen as the terminal, and the anionic alkoxo-oxygen atom

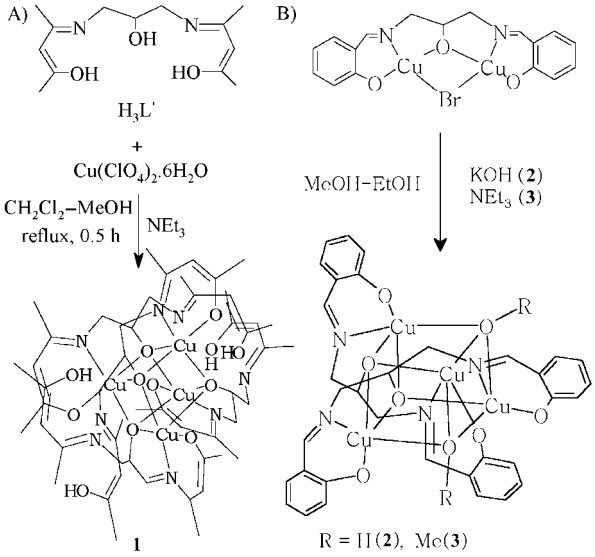

Scheme 1. Synthetic routes to complex **1** (A) and complexes **2** and **3** (B).

Table 1. Selected bond lengths [Å] and angles [°] for $1\cdot 4H_2O$.[a]

Cu1···Cu1(#1)	3.124(2)	O(1)–Cu(1)–N(1)	94.9(3)
Cu1···Cu1(#2)	3.438(1)	O(1)–Cu(1)–O(2)	179.6(3)
Cu1–O1	1.905(6)	O(2)-Cu(1)-N(1)	85.0(3)
Cu1–O2(#1)	1.971(5)	O(1)-Cu(1)-O(2)#2	102.3(2)
Cu1–O2	1.974(5)	O(1)-Cu(1)-O(2)#1	92.7(2)
Cu1–O2(#2)	2.437(5)	O(2)#1-Cu(1)-N(1)	170.4(3)
Cu1–N1	1.927(7)	O(2)#2-Cu(1)-N(1)	108.5(2)
Cu1-O2-Cu1(#1)	104.7(2)	O(2)-Cu(1)-O(2)#1	87.4(2)
Cu1-O2(#1)-Cu1(#1)	89.6(2)	O(2)-Cu(1)-O(2)#2	78.0(2)
Cu1-O2-Cu1(#2)	101.9(2)	O(2)#1-Cu(1)-O(2)#2	75.5(2)

[a] Symmetry codes: #1; $-x+3/2$, $-y+1/2$, $z-1/2$; #2: x, $-y$, $-z+1$

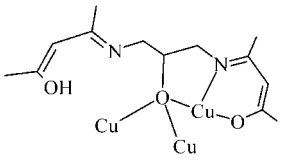

A

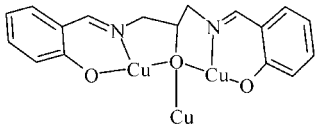

B

as the bridging site (**A**). The alkoxo-oxygen atom that belongs to the amine part of the ligand links two copper(II) centers in an axial–equatorial fashion. The copper centers are in an essentially square-pyramidal (4+1) geometry with one bridging Cu–O bond as the axial ligand [distance, 2.437(5) Å]. The elongation of the Cu–O axial bond is due to a pseudo-Jahn–Teller distortion of the d^9 Cu center. The metal atom in the structure shows a deviation of about 0.05 Å from the NO_3 basal plane. The dihedral angle between the two coordination planes containing the Cu1 and Cu1(#2) atoms is approximately 31°. The dihedral angle between the planes containing the Cu1 and Cu1(#1) atoms is about 86°. The Cu1···Cu1(#1) distance is 3.124(2) Å. The axial–equatorial alkoxo oxygen atom bridges the Cu1 and Cu1(#2) atoms with a separation of 3.438(1) Å. The O2 bridging atom in **1**, which shows a pyramidal geometry with the sum of the angles C7–O2–Cu1, C7–O2–Cu1(#1), and Cu1–O2–Cu1(#1) of about 337°, is likely to reduce the magnitude of the antiferromagnetic coupling between the copper centers.[20,21] This complex has a 1:1 ratio of copper and the ligand. As the potentially pentadentate ligand only binds to the metal in a tridentate mode in **1**, this means that two free donor sites are available per ligand, making eight in total per cubane cluster, for further metal binding. As a consequence, this complex is reactive and behaves like a "molecular octopus" with eight pendant binding sites suitable for cluster expansion through a metal-driven, self-assembly process, as observed in the isolation of a metallomacrobicyclic octanuclear copper(II) and a mixed valent tetradecanuclear $Cu^{II}_{12}Cu^{I}_{2}$ cluster with a prismatic structure from complex **1** (Scheme 2).[15,23] In an alcoholic KOH medium, the complex reacts with copper(II) perchlorate, in the absence of any additional H_3L', to form four binuclear units that are linked by one μ_2-OH and two μ_3-OH ligands to form the octanuclear core. Addition of H_3L' in a similar reaction in the

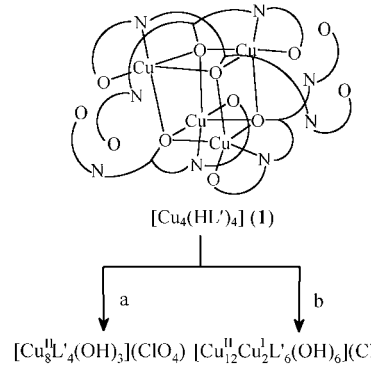

Scheme 2. Reaction pathways involved in the self-assembly processes forming the octa- and tetradecanuclear copper cores from complex **1** (0.16 mM): a) $[Cu(H_2O)_6](ClO_4)_2$ (0.64 mM) and KOH (0.94 mM) in EtOH (15 mL); b) $[Cu(H_2O)_6](ClO_4)_2$ (1.6 mM), H_3L' (0.64 mM) and piperidine (1.5 mM) in CH_2Cl_2/MeOH (20 mL, 1:1 v/v).

presence of piperidine, however, gives a mixed-valent tetradecanuclear core in which the steric restrictions lead to the reduction of two copper(II) ions to copper(I).

The cubane complex **2** with the formula $[Cu_4L_2(OH)_2]\cdot 6H_2O$ ($\mathbf{2}\cdot 6H_2O$) belongs in the orthorhombic space group *Pccn* and contains six water molecules per tetramer. The complex $[Cu_4L_2(OMe)_2]$ (**3**) also crystallizes in the same space group but with one THF and two H_2O lattice molecules per cluster unit. The ORTEP views of complexes **2** and **3** are shown in Figure 2 and Figure 3, respectively. Selected bond lengths and angles are given in Table 2. The complexes have a Cu_4O_4 cubane core in which the bridging oxygen atoms come from two Schiff bases, each of which provides one alkoxo-oxygen atom; the remaining two oxygen atoms come from hydroxo groups for **2** and methoxy groups for **3**. The copper(II) atoms are in a square-pyramidal environment with NO_4 coordination. Both structures can be viewed as two $\{Cu_2L\}^+$ units self-assembled to form the

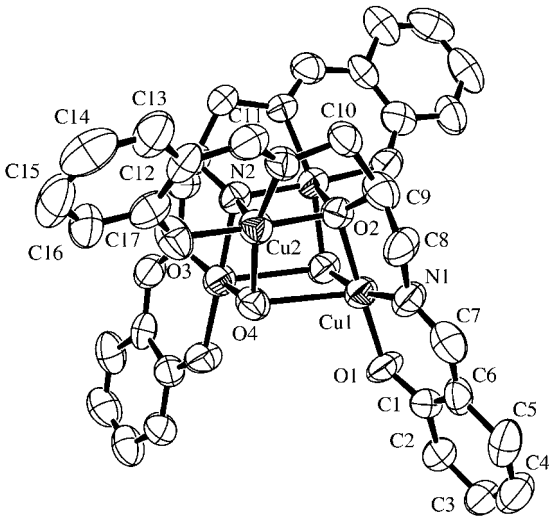

Figure 2. Molecular structure of $[Cu_4L_2(OH)_2]\cdot 6H_2O$ ($\mathbf{2}\cdot 6H_2O$) displaying (ORTEP view; 50% probability thermal ellipsoids).

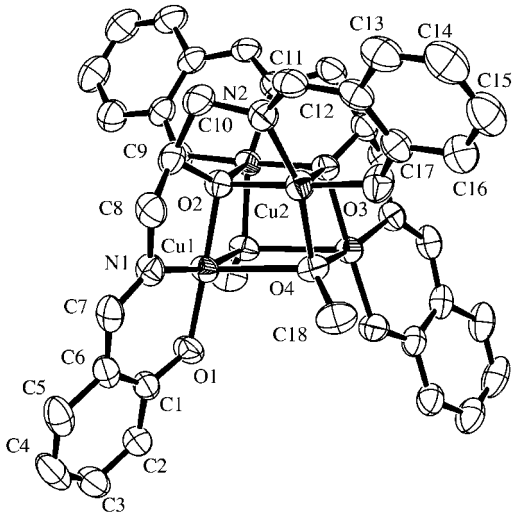

Figure 3. Molecular structure of $[Cu_4L_2(OMe)_2]\cdot 2H_2O\cdot THF$ (**3**·2 H_2O·THF) (ORTEP view; 50% probability thermal ellipsoids).

cubane core in the presence of two μ_3-OH or μ_3-OMe ligands. The trianionic ligand shows a pentadentate mode of coordination in **2** and **3** (**B**).

Complex **2** has an average equatorial Cu–O bond length of 1.97 Å and an average axial Cu–O bond length of 2.43 Å. The Cu1···Cu2 and Cu1(#1)···Cu2 distances in **2** involving copper atoms linked by equatorial alkoxo oxygen atoms are 3.103(2) and 3.107(2) Å, respectively. The Cu1···Cu1(#1) and Cu2···Cu2(#1) distances for axial–equatorial bridged copper(II) atoms are 3.433(2) and 3.458(2) Å, respectively. The Cu-O-Cu angles for the equatorially bridged copper atoms are 105.8(5)° and 104.3(4)°. The other Cu-O-Cu angles for the copper atoms bridged in an axial–equatorial fashion are in the range 103.5(3)–88.8(3)°. The dihedral angle between the planes containing the Cu1 and Cu2 atoms is 87.6(3)° and that for the planes containing the Cu1 and Cu2A atoms is 82.7(3)°. The equatorial–equatorial and equatorial–axial dibridged coordination planes of the pairs of copper atoms Cu1(#1),Cu2 and Cu1(#1),Cu(#2) make angles of 63.2(2)° and 74.0(2)°, respectively, between themselves. The dihedral angles between the copper atoms having only axial–equatorial-type bridges are less than those having both equatorial–equatorial or axial–equatorial bridges. The geometry of the bridging alkoxo and hydroxo oxygen atoms O2 and O4 varies between pyramidal (~323°) and nearly planar (~347°) conformations.

The structural features of complex **3** are essentially the same as those of **2.** The average Cu–O distance in the square plane is 1.97 Å. The axial bonds show a distance of 2.476(3) Å for Cu1–O4(#1) and 2.318(2) Å for Cu2–O2. The Cu-O-Cu angles are in the range 104.0(1)–88.3(1)°. The distances for the equatorially oxygen-bridged copper atoms Cu1,Cu2 and Cu1,Cu2(#1) are 3.077(1) and 3.116(1) Å, respectively. The Cu-O-Cu angles involving these pairs of copper atoms are 104.0(1)° and 103.8(1)°, respectively. The planes containing oxygen-bridged copper atoms with short Cu–O distances are nearly perpendicular to each other, whereas the planes containing the Cu1 and Cu2 atoms lie at a dihedral angle of 88.9(1)°. The dihedral angle between the planes containing the Cu1 and Cu2(#1) atoms is 83.2(1)°. The dihedral angles between the axial–equatorial-bound copper planes of Cu1,Cu1(#1) and Cu2,Cu2(#1) are 37.5(1)° and 24.7(1)°, respectively. The geometry of the bridging oxygen atoms O2 and O4 in **3** is similar to that in complex **2**.

The crystal structures of **1**–**3** exhibit chemically significant hydrogen-bonding interactions between the complexes and the lattice solvent molecules (see Figure S1–S3 in the Supporting Information). In complex **1**, the solvent water molecule is involved in hydrogen-bonding interactions with the pendant group of the Schiff base (2.61(2) Å; O3–H31···O4 angle of 145.9(9)°). The O5···O5(#4) distance of 2.73(4) Å indicates strong intermolecular hydrogen-bonding interac-

Table 2. Selected bond lengths [Å] and angles [°] for complexes **2**·6 H_2O[a] and **3**·2 H_2O·THF.[b]

	2·6 H_2O	**3**·2 H_2O·THF
Cu1···Cu2	3.103(2)	3.077(1)
Cu1···Cu2(#1)	3.108(2)	3.116(1)
Cu1···Cu1(#1)	3.433(2)	3.419(1)
Cu2···Cu2(#1)	3.458(3)	3.384(1)
Cu1–O1	1.897(8)	1.885(2)
Cu1–O2	1.966(8)	1.961(2)
Cu1–O4	1.926(10)	1.948(2)
Cu1–O4(#1)	2.451(8)	2.476(3)
Cu1–N1	1.921(12)	1.937(3)
Cu2–O2	2.418(8)	2.318(2)
Cu2–O4	1.964(9)	1.961(2)
Cu2–O2(#1)	1.969(8)	1.992(2)
Cu2–O3	1.910(9)	1.888(3)
Cu2–N2	1.914(10)	1.938(3)
Cu1-O2-Cu2	89.5(3)	91.6(1)
Cu1-O4-Cu2	105.8(5)	103.8(1)
Cu1-O2-Cu2(#1)	104.3(4)	104.0(1)
Cu1(#1)-O4-Cu2	88.8(3)	88.3(1)
Cu2-O2-Cu2(#1)	103.5(3)	103.2(1)
Cu1-O4-Cu1(#1)	102.7(3)	100.4(1)
O1-Cu1-O2	178.2(4)	177.2(1)
O1-Cu1-O4	94.6(4)	96.9(1)
O1-Cu1-O4(#1)	105.4(4)	104.9(1)
O1-Cu1-N1	95.1(4)	94.0(1)
O2-Cu1-O4	87.1(4)	85.9(1)
O2-Cu1-O4(#1)	75.4(3)	75.9(1)
O2-Cu1-N1	83.2(4)	83.2(1)
O4-Cu1-O4(#1)	77.3(4)	79.5(1)
O4-Cu1-N1	166.3(4)	164.2(1)
O4(#1)-Cu1-N1	109.3(4)	108.7(1)
O4-Cu2-O2(#1)	87.8(4)	88.4(1)
O2-Cu2-O2(#1)	76.4(3)	76.9(1)
O2-Cu2-O3	104.3(4)	104.3(1)
O2-Cu2-O4	74.6(4)	76.5(1)
O2(#1)-Cu2-O3	177.2(4)	177.2(1)
O2(#1)-Cu2-N2	83.3(4)	83.4(1)
O2-Cu2-N2	119.1(4)	117.9(1)
O3-Cu2-O4	95.0(4)	94.3(1)
O3-Cu2-N2	94.0(4)	93.9(1)
O4-Cu2-N2	161.0(4)	160.9(1)

[a] Symmetry code: #1; $-x+1/2$, $-y+1/2$, $+z$. [b] Symmetry code: #1; $-x+3/2$, $-y+1/2$, z.

tions between the water molecules (symmetry code #4: $-x+1, +y, -z+1$). The hydroxo oxygen atom O4 of **2** lies at a distance of 3.07(2) Å from the disordered solvent water molecule O5 (O4–H···O5 angle: ~160°). The positionally disordered water molecules showing intermolecular distances of 2.6–2.9 Å among themselves are located within the nearly strawberry-shaped channel with a cross-section of around 8×6 Å along the crystallographic *a* axis. The water molecules are also present in the zigzag channel that propagates along the crystallographic *b* axis. The lattice solvent molecules in **3** are tetrahydrofuran and water. They are located in the channel possessing a similar area of cross-section to that of **2** along the crystallographic *a* axis. The water molecules of complex **3** show significant hydrogen-bonding interactions (O5···O6: 2.689(7) Å). The water molecule O6 exhibits possible intermolecular hydrogen-bonding interactions with the phenoxo oxygens O1(#5) and O1(#6) of the pentadentate Schiff-base ligand, with an O6···O1 distance of 2.790(4) Å and O1(#5)···O6···O1(#6) angle of about 102°.

Magnetic properties: The temperature dependence of the magnetic susceptibility of cubane cluster **1** is shown as a $\chi_M T$ versus T plot in Figure 4. The value of $\chi_M T$ remains nearly

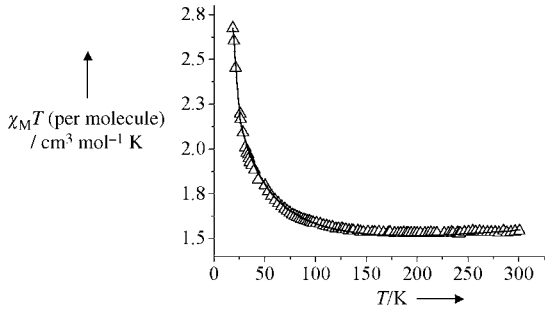

Figure 4. A plot of $\chi_M T$ versus T for a polycrystalline sample of $[Cu_4(HL')_4]$ (**1**). The solid line is the theoretical fit to the experimental data.

constant from 300 K to about 120 K ($\approx 1.55\ cm^3 mol^{-1} K$) and thereafter gradually increases to a value of $2.67\ cm^3 mol^{-1} K$ (at 18 K) as the temperature is lowered steadily. The μ_{eff} value is 3.51 μ_B at 300 K and 4.63 μ_B at 18 K, which is marginally smaller than the magnetic moment of 4.90 μ_B for a molecule in the ground state with a total spin of 2 (spin-only value, assuming that the *g* factor is 2). The magnetic data show that the effective exchange interactions between the copper(II) spins in cubane **1** are ferromagnetic.

To determine the nature of the individual exchange interactions, we noted that the copper(II) ions occupy alternate cube corners in these systems. Thus, there are six exchange interactions between the four magnetic ions in the molecules (Scheme 3). The symmetry of cubane **1** (Figure 1) further reduces these to two unique exchange constants, with four of the six exchange constants having one unique value (J_1) and the remaining two exchange constants the other

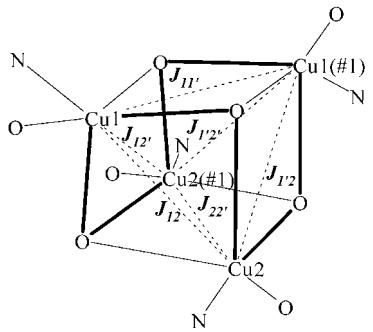

Scheme 3. Magnetic exchange pathways for the cubane core in complexes **1**–**3** with the short Cu–O bonds shown by thick lines.

(J_2). The Cu–O–Cu bond angles for the exchange pathway involving J_1 are nearly 90° while the Cu–O–Cu bond angles for the exchange pathway involving J_2 are above 100° (ca. 101.9°). This implies that J_1 is ferromagnetic while J_2 could be antiferromagnetic. Furthermore, the Cu–O and Cu···Cu distances for the different pathways are consistent with $|J_1| > |J_2|$. The oxygen atoms involved in the superexchange interaction are arranged in a pyramidal geometry around the copper ions, the sum of the bond angles around the copper ion being about 337°. It is empirically known that such a pyramidal arrangement of ligand atoms leads to an increase in the strength of ferromagnetic interactions and a decrease in the strength of antiferromagnetic interactions.[20,21,35] Based on these structural and magnetic data, we modeled the magnetic interactions in cubane **1** using the Hamiltonian in Equation (4), where a positive sign of J corresponds to a ferromagnetic interaction and a negative sign of J to an antiferromagnetic interaction. All the spin operators (S) correspond to spin-1/2 objects. The last term in the Hamiltonian takes into account intermolecular interactions within the mean-field approximation. This is necessary since high-spin molecules experience intermolecular dipolar interactions, which can be represented by a weakly ferromagnetic or antiferromagnetic exchange term. Thus, $|J'| \ll \{|J_1|, |J_2|\}$ and the strength of the effective interaction depends upon the number of nearest neighbor molecules, z, which in the case of cubane **1** is six, while for cubanes **2** and **3** it is four.

$$H = -J_1(\hat{S}_1\hat{S}_2 + \hat{S}_1\hat{S}_{2'} + \hat{S}_{1'}\hat{S}_{2'} + \hat{S}_{1'}\hat{S}_2) - J_2(\hat{S}_1\hat{S}_{1'} + \hat{S}_2\hat{S}_{2'}) + g\mu_B H \sum_i \hat{S}_i^z - zJ' < S^z_{tot} > \sum_i \hat{S}_i^z \quad (4)$$

Using the above model we can compute the square of the magnetization, $M^2(T)$, as a function of temperature as given in Equation (5), where the eigenvalues $E(S,M_s)$ of H are given by $E(S,M_s) = E_o(S,M_s) + M_s(g\beta H - zJ' < S_z >)$, with $E_o(S,M_s)$ being the eigenvalues of the exchange Hamiltonian in the absence of external magnetic field and intermolecular interactions.

$$M_2(T) = \frac{\sum_S \sum_{Ms=-S}^{S} M_S{}^2 \exp(-E(S,M_S)/k_BT)}{\sum_S \sum_{Ms=-S}^{S} \exp(-E(S,M_S)/k_BT)} \quad (5)$$

The temperature-dependent magnetic susceptibility, $\chi_M(T)$ is then given by Equation (6), where g is the gyromagnetic ratio.

$$\chi_M(T) = g^2 M^2(T)/[T - zJ'M^2(T)] \quad (6)$$

To account for trace amounts of paramagnetic impurity present in the analytically pure sample, an additional Curie-like contribution to the magnetic susceptibility was assumed and the total magnetic susceptibility is then given by Equation (7), where C is the Curie constant.

$$\chi_{tot}(T) = \chi_M(T) + C/T \quad (7)$$

The error in the fit (R) was calculated from expression (8), where $\chi_{obs}(T_i)$ and $\chi_{cal}(T_i)$ are the observed and calculated magnetic susceptibilities at temperature T_i, respectively.

$$R = \sum_i [\{\chi_{obs}(T_i) - \chi_{cal}(T_i)\}^2/\chi_{obs}(T_i)^2] \quad (8)$$

The best fit J_1, J_2, and J' values for cubane **1** are 38.4, −18.0, and 0.14 cm^{-1} respectively. In all these calculations a g value of 2.01 was used. The Curie constant obtained from the fit corresponds to an impurity concentration of 0.03 free-spins per cubane cluster. The error (R) found for the fit is 1.22×10^{-4}.

Interestingly, the intermolecular exchange interaction determined from the fit is ferromagnetic in **1**. The energy levels computed by using the above intramolecular exchange parameters for an isolated cubane molecule yield a triplet ground state (Figure 5). The fact that the ground state is neither the high-spin quintet state nor the low-spin singlet state, but an intermediate spin-one state, is an outcome of the presence of both ferro- and antiferromagnetic exchange interactions. The lowest excited state is a quintet state, with a singlet state lying above the quintet. The triplet–quintet gap is 7.88 cm^{-1} and the triplet–singlet gap is 38.43 cm^{-1}. It

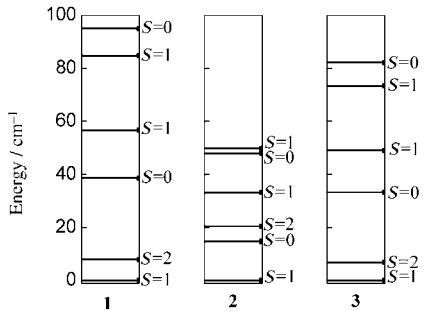

Figure 5. The energy-level diagrams of complexes **1**–**3** with a degeneracy of $(2S+1)$ for each spin state. The spin of each state is indicated to the right.

appears that the internal magnetic field due to ferromagnetic intermolecular interactions lowers the quintet state energy and brings it closer to the triplet ground state. This explains the increase in the μ_B value close to $S=2$ at low temperatures.

Cubane **2** has a μ_{eff} value of 2.98 μ_B at 300 K and 3.64 μ_B at 18 K. The temperature dependence of the magnetic susceptibility is shown as a $\chi_M T$ versus T plot in Figure 6. The

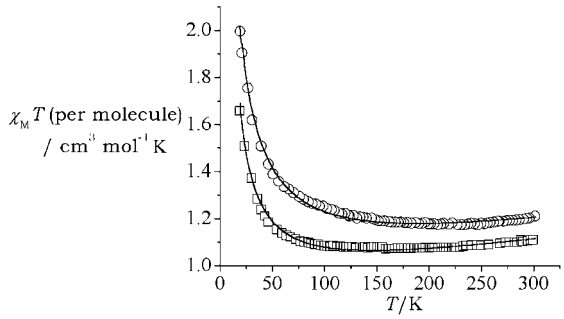

Figure 6. Plots of $\chi_M T$ versus T for the polycrystalline samples of **2** (□) and **3** (O) with solid lines showing the theoretical fit to the experimental data.

change of the magnetic susceptibility with temperature is similar to that of cubane **1** over the entire range of temperature. The Cu-O-Cu bond angles and also the Cu–O and Cu···Cu bond lengths of cubane **2** are similar to those of cubane **1** except that the axial bonds which involve the exchange parameter J_2 are elongated (above 2.4 Å) due to a pseudo-Jahn–Teller distortion. Hence, a weaker exchange constant is expected for J_2. The oxygen atoms involved in the superexchange interaction are nearly planar to pyramidal, with the sum of the bond angles around the copper(II) ion varying between 325° and 354°. The best-fit values for J_1, J_2, and J' are 14.7, −18.4, and 0.43 cm^{-1}, respectively, with $g=2.04$ and $R=5.5\times10^{-5}$; the paramagnetic impurity concentration is of 0.01 free-spins per cubane cluster.

The intermolecular exchange interaction in cubane **2** is also ferromagnetic. The ground state of cubane **2** is also a triplet due to the presence of both ferro- and antiferromagnetic exchange interactions in the system. However, unlike cubane **1**, the lowest excited state is a singlet with a quintet state lying above it (Figure 5). The triplet–singlet gap is 14.70 cm^{-1} and the triplet–quintet gap is 20.34 cm^{-1}. Indeed, it is well known that it is difficult to predict, a priori, either the ground state spin or the ordering of the excited states in spin systems.

Cubane **3** has a μ_{eff} value of 3.11 μ_B at 300 K and 4.02 μ_B at 18 K. The temperature dependence of the magnetic susceptibility is shown as a $\chi_M T$ versus T plot in Figure 6. The plot shows the magnetic behavior of the complex, which is similar to those of cubanes **1** and **2**. The Cu-O-Cu bond angles are comparable to those of cubane **2**. As in cubane **2**, the axial bonds are elongated (2.32 Å and 2.48 Å) due to a pseudo-Jahn–Teller distortion. Moreover, the cubane cluster

3 involves all the alkoxo-oxygen atoms as bridging groups, whereas in cubane **2** there are two alkoxo and two hydroxo groups. It is well known from the literature that the critical angle for having a ferromagnetic exchange pathway is higher for alkoxo-oxygen atoms.[36] Since cubane **3** has only alkoxo groups, the ferromagnetic exchange coupling for cubane **3** is expected to be higher than for cubane **2**. The value of the exchange constant obtained using the model discussed earlier for the ferromagnetic pathway is $J_1 = 33.3\ cm^{-1}$ and that for the antiferromagnetic pathway is $J_2 = -15.6\ cm^{-1}$. The intermolecular interaction parameter obtained was $J' = 0.25\ cm^{-1}$, which is indeed ferromagnetic. The error, R, in the fit is 1.02×10^{-5}, with a g value of 2.02 and a paramagnetic impurity concentration of 0.04 free-spins per cubane cluster. The calculated energy-level diagram using the J_1 and J_2 values yields a spin triplet ground state with a quintet excited state at $6.76\ cm^{-1}$ and a singlet excited state at $33.3\ cm^{-1}$ (Figure 5).

Magnetostructural correlations: Cubane copper(II) clusters with a magnetic ground state are of importance as new magnetic systems; such cubane clusters are listed in Table 3 for comparison of their magnetostructural properties.[16–23] Ito and co-workers have reported a copper(II) cubane $[Cu_4(hase)_4]\cdot 2H_2O\cdot 4MeCN$ which shows ferro- and antiferromagnetic exchange interactions with exchange parameter values of 72.2(2) and $-35.2(2)\ cm^{-1}$, respectively. This complex, which displays a channel structure with the solvent molecules located within the channel, has average Cu–O distances of 1.95 and 2.51 Å for the equatorial and axial bonds respectively.[20] The Cu-O-Cu angles are 105.5° and 95.4°. Nakano and co-workers have designed an open, cubane-like Cu_4O_4 complex of formula $[Cu_4(hpda)_4](ClO_4)_4\cdot H_2O$ (Hhpda: *N*-(2-hydroxyethyl)-1,3-propanediamine) that shows ferromagnetic interactions.[21] The square planes of the copper atoms in this complex have dihedral angles of 82.58° and 96.57°, which suggests that the $d_{x^2-y^2}$ magnetic orbitals of the metal centers are nearly perpendicular to each other thereby promoting a ferromagnetic interaction ($2J = 89.8\ cm^{-1}$). Complexes **1**–**3** also show dihedral angles between the copper(II) planes of about 90°. Such a structural feature is in accordance with the ferromagnetic behavior of these complexes. Complex **1** has significant structural differences from its analogues, which make it more ferromagnetic than **2** and **3**.

Conclusion

Complexes **1**–**3** are the first structurally characterized copper(II) cubanes with a magnetic triplet ($S = 1$) ground state. The nature of the magnetic coupling in **1**–**3** is significantly different from the majority of the reported copper(II) cubanes,[24–34] which are antiferromagnetic in nature, but resembles those having a quintet ground state.[16,19] The intramolecular ferromagnetic interaction could be due to the orthogonality of the magnetic orbitals for at least one exchange pathway in each copper pair. Complexes **2** and **3** are formed from a dimeric precursor with a hydroxo or alkoxo group, which facilitates the self-assembly process. Cubane **1** has eight pendant binding sites that are suitable for a cluster-expansion process in the presence of additional metal ions. It is a potential precursor for the synthesis of discrete, high-nuclearity clusters of nanometer size.

Table 3. Structurally characterized cubane copper(II) clusters with a magnetic ground state.

No.	Complexes	$Cu-O_{eq}$ [Å] $Cu-O_{ax}$ [Å]	Cu–O–Cu [°]	J [cm^{-1}]	Ref.
1	$[Cu_4Br_4(CH_2CH_2NEt_2)_4]\cdot 4CCl_4$	1.92–1.98 2.52	104.1; 108.8; 88.8	−9.0(3); 80.0(3)	[16b]
2	$[Cu_4(MeCOCHCMe{=}NCH_2CH_2O)_4]$	1.92–1.97 2.33–2.69	109.8–87.3	−19.8(6.0); 41.0(6.0)	[17]
3	$[Cu_4(L^1)_4]\cdot 9MeOH$[a]	1.96–2.00 2.48	104.4; 99.0; 88.8	57(4); −14(4)	[18]
4	$[Cu_4(L^2)_4]\cdot 8EtOH$[b]	1.94–1.99 2.75	112.0; 94.4; 86.1	0; 34.8	[18]
5	$[Cu_4(bpy)_4(OH)_4](PF_6)_4$[c]	1.95–1.96 2.49	105.0–90.8	15.1; 0.16	[19]
6	$[Cu_4(hsae)_4]\cdot 2H_2O\cdot 4MeCN$[d]	1.93–2.0 2.56	106.1–85.8	−35.2(2); 72(2)	[20]
7	$[Cu_4(hpda)_4](ClO_4)_4\cdot H_2O$[e]	1.92–1.99	110.0; 108.9, 108.0, 110.1	−32.6; 89.8	[21]
8	$[Cu_4(L^3)_4]$[f]	1.90–1.97 2.41–2.51	107.7–88.8	−9.4(4); 15.2(4)	[22]
9	$[Cu_4(HL')_4]\cdot 4H_2O$	1.91–1.97 2.44	104.7; 101.9; 89.6	38.5; −18	this work
10	$[Cu_4L_2(OH)_2]\cdot 6H_2O$	1.93–1.97 2.42–2.45	105.8–88.8	14.7; −18.4	this work
11	$[Cu_4L_2(OMe)_2]\cdot 2H_2O\cdot THF$	1.95–1.99 2.32 −2.48	104.0–88.3	33.3; −15.6	this work

[a] H_2L^1: Schiff base of pyridoxal and 2-amino-1-phenylpropan-1-ol. [b] H_2L^2: Schiff base of pyridoxal and 2-amino-1-phenylethanol. [c] bpy: 2,2′-bipyridine. [d] H_2hsae: 2-(4-hydroxysalicylidineamino)ethanol. [e] Hhpda: *N*-(2-hydroxyethyl)-1,3-propanediamine. [f] H_2L^3: ethyl-2-[*N*-(2-hydroxycyclohexyl)aminomethylene]-3-oxobutanoate.

Experimental Section

Materials and measurements: All reagents and chemicals were purchased form commercial sources and used without further purification. The Schiff bases *N*,*N*′-(2-hydroxypropane-1,3-diyl)bis(salicylaldimine) (H_3L) and *N*,*N*′-(2-hydroxypropane-1,3-diyl)bis(acetylacetoneimine) (H_3L') were prepared by literature methods.[37] The precursor complex $[Cu_2LBr]$ was synthesized from H_3L and $CuBr_2\cdot H_2O$ by following a procedure similar to that reported for an analogous dinuclear copper(II) complex of the Schiff-base ligand *N*,*N*′-(2-hydroxypentane-1,5-diyl)bis(salicylaldimine).[38] The elemental analyses were performed with a Heraeus CHN-O Rapid instrument.

The electronic and IR spectral data were obtained with Perkin Elmer Lambda 35 and Bruker Equinox 55 spectrometers, respectively. The variable-temperature magnetic susceptibility measurements were performed with a Model 300 Lewis-coil-force magnetometer (George Associates Inc., Berkeley, CA) equipped with a closed-cycle cryostat (Air products) and a Cahn balance. $Hg[Co(NCS)_4]$ was used as a standard. Experimental susceptibility data were corrected for diamagnetic contributions ($\chi_{dia} = -95.3\times10^{-6}\,cm^3\,M^{-1}$ per copper atom). The magnetic moments at various temperatures were calculated in μ_B unit [$\mu_B \approx 9.274\times10^{-24}\,J\,T^{-1}$].

Synthesis of $[Cu_4(HL')_4]$ (1): Triethylamine (3.9 mL, 28.03 mmol) was added to a solution of H_3L' (3.79 g, 14.9 mmol) in dichloromethane (20 mL) with magnetic stirring. After 10 min a solution of $[Cu(H_2O)_6](ClO_4)_2$ (2.96 g, 8.0 mmol) in MeOH (20 mL) was added dropwise. The mixture was then heated to reflux for 30 min. The solution was cooled to ambient temperature and its volume was reduced to half on a rotary evaporator. A dark-blue, crystalline solid of **1** (2.2 g, yield ~87%) separated on standing overnight. This solid was isolated, washed with a cold methanol/diethyl ether solvent mixture (1:1, v/v), and finally dried in vacuum over fused $CaCl_2$. Elemental analysis (%) calcd for **1** ($C_{52}H_{40}Cu_4N_8O_{12}$ (1263.4)): C 49.44, H 6.38, N 8.87; found: C 49.21, H 6.54, N 9.02; IR (KBr phase): $\tilde{\nu}$ = 3403w, 2987w, 2950w, 2921w, 2866w, 2822w, 1615s, 1564s, 1500s, 1462w, 1439m, 1407s, 1351w, 1300m, 1281m, 1212w, 1102w, 1034w, 1044w, 945w, 737m, 617m, 437w cm^{-1}; UV/Vis (MeOH): λ_{max} (ε) = 233 (22500), 310 (43000), 630 nm (280 $M^{-1}cm^{-1}$).

Synthesis of $[Cu_4L_2(OH)_2]$ (2): A 1.0 M ethanolic solution of KOH was added dropwise to a solution of $[Cu_2LBr]$ (0.45 g, 0.89 mmol) in methanol (20 mL) until the solution turned dark green. The resulting solution was heated in a water bath for 30 min. It was then cooled to room temperature and filtered to remove any solid present in the solution. The green filtrate gave dark green, crystalline **2** on standing overnight. This solid was isolated, washed with cold methanol, and dried in vacuum over P_4O_{10} [Yield: 0.47 g (59%)]. Elemental analysis (%) calcd for **2** ($C_{34}H_{32}Cu_4N_4O_8$ (878.9)): C 46.47, H 3.67, N 6.37; found: C 45.16, H 3.72, N 6.43; IR (KBr phase): $\tilde{\nu}$ = 3392br, 3191br, 3050w, 2911w, 2886w, 2833w, 1640s, 1602m, 1582m, 1540s, 1468m, 1453s, 1395s, 1345m, 1314s, 1199m, 1178m, 1156m, 1130m, 1069w, 1049w, 1033w, 986w, 971w, 553w, 464m cm^{-1}; UV/Vis (MeOH): λ_{max} (ε) = 242 (49500), 269 (32200), 362 (11500), 639 nm (360 $M^{-1}cm^{-1}$).

Synthesis of $[Cu_4L_2(OMe)_2]$ (3): Triethylamine (0.15 mL, ~1.0 mmol) was added slowly to a methanolic solution (25 mL) of $[Cu_2LBr]$ (0.5 g, 0.99 mmol). After stirring for 8 h the solution was filtered to remove any insoluble material. The filtrate was concentrated on a rotary evaporator and the solid thus obtained was isolated and washed with cold methanol. The crude product was then crystallized from a tetrahydrofuran/methanol mixture (1:2, v/v). The solid obtained was dried in vacuum over P_4O_{10} for analytical studies. Yield: 0.45 g (~55%). Elemental analysis (%) calcd for **3** ($C_{36}H_{36}Cu_4N_4O_8$ (906.8)): C 47.63, H 4.00, N 6.17; found: C 46.21, H 3.95, N 6.24; IR (KBr phase): $\tilde{\nu}$ = 3356br, 2918w, 2872w, 2808w, 1640s, 1602m, 1539m, 1448s, 1395m, 1345m, 1312s, 1199m, 1148m, 1125m, 1044m, 1027m, 977w, 893m, 861m, 759s, 717w, 563m cm^{-1}; UV/Vis (MeOH): λ_{max} (ε) = 245 (51000), 273 (32800), 368 (12000), 642 nm (380 $M^{-1}cm^{-1}$).

X-ray crystallographic studies: Single crystals of **1** were obtained by slow evaporation of a solution of the complex. A crystal of approximate size $0.27\times0.18\times0.15\,mm^3$ was mounted on a glass fiber using epoxy cement. The X-ray diffraction data were measured in frames with increasing ω (width of 0.3° per frame) at a scan speed of 6 s/frame using a Bruker SMART APEX CCD diffractometer, equipped with a fine-focus, sealed-tube X-ray source. The SMART software was used for data acquisition and the SAINT software for data extraction.[39a] Empirical absorption corrections were made on the intensity data.[39b] The structure was solved by the heavy atom method and refined by full-matrix least-squares with the SHELX system of programs.[40] All non-hydrogen atoms of the complex, except those of the solvent water molecules, were refined anisotropically. All the hydrogen atoms were generated, assigned isotropic thermal parameters, and refined using a riding model. The hydrogen atoms were used for the structure factor calculation only. The positionally disordered oxygen atoms O4 and O5 of the solvent water molecules in the asymmetric unit were refined with a site occupancy factor of 0.5. The structure refinement gave a goodness-of-fit (GoF) value of 1.077 with a maximum shift/esd value of 0.001.

Single crystals of **2** were obtained by slow concentration of a methanolic solution of the complex. A green crystal of **2**·6H_2O of size $0.25\times0.2\times0.1\,mm^3$ was mounted on a glass fiber with epoxy cement and all geometric and intensity data were collected with an automated Enraf-Nonius CAD4 diffractometer fitted with $Mo_{K\alpha}$ radiation. Intensity data, collected using the ω-scan technique for 3711 reflections in the range $1.6 \le \theta \le 25.0°$, were corrected for Lorentz-polarization effects and for absorption.[41] Of 2545 unique data, 1617 with $I \ge 2\sigma(I)$ were used for structure determination involving 252 parameters, which gave a goodness-of-fit value of 1.053 and highest shift/esd value of 0.0. All non-hydrogen atoms except the solvent oxygen atoms were refined anisotropically. The hydrogen atom attached to the oxygen atom O4 was located from the difference Fourier map and refined isotropically using geometrical restraints available within the SHELX program, while those attached to the carbon

Table 4. Crystallographic data for the complexes $[Cu_4(HL')_4]\cdot4H_2O$ (**1**·4H_2O), $[Cu_4L_2(OH)_2]\cdot6H_2O$ (**2**·6H_2O) and $[Cu_4L_2(OMe)_2]\cdot2H_2O\cdot$THF (**3**·2$H_2O$·THF).

	1·4H_2O	**2**·6H_2O	**3**·2H_2O·THF
chemical formula	$C_{52}H_{88}Cu_4N_8O_{16}$	$C_{34}H_{44}Cu_4N_4O_{14}$	$C_{40}H_{48}Cu_4N_4O_{11}$
M_r	1335.46	986.89	1014.98
crystal system	cubic	orthorhombic	orthorhombic
space group	$P\bar{4}3n$	$Pccn$	$Pccn$
unit cell dimensions			
a [Å]	22.421	9.292(3)	8.9080(10)
b [Å]	22.421	18.066(4)	18.026(2)
c [Å]	22.421	25.134(5)	25.942(5)
α [°]	90	90	90
β [°]	90	90	90
γ [°]	90	90	90
V [Å^3]	11272(3)	4219.2(19)	4165.7(10)
Z	6	4	4
crystal size [mm^3]	0.27×0.18×0.15	0.25×0.2×0.1	0.24×0.15×0.1
min/max trans.	0.63/0.83	0.49/0.72	0.57/0.79
ρ_{calcd} [g cm^{-3}]	1.180	1.554	1.618
μ ($Mo_{K\alpha}$) [cm^{-1}]	11.74	20.55	20.79
T [K]	293(2)	293(2)	293(2)
reflections collected	2960	3711	29852
unique reflections	2960	3711	4086
variables	180	252	348
R(int)	0.1554	0.0	0.1282
reflections used for refinement [$F_o^2 > 2\sigma(F_o^2)$]	2244	1617	2996
$R1$[a]	0.0693	0.0889	0.0371
$wR2$[b]	0.1805	0.2078	0.0918
$\Delta\rho_{max}$ [e Å^{-3}]	0.704	0.835	0.484
$\Delta\rho_{min}$ [e Å^{-3}]	−0.405	−0.449	−0.350

[a] $R = \Sigma\,||F_o| - |F_c||/\Sigma\,|F_o|$. [b] $wR = \{\Sigma[w(F_o^2 - F_c^2)^2]/\Sigma[w(F_o^2)^2]\}^{1/2}$. $w = 1/[\sigma^2(F_o^2) + (AP)^2 + BP]$ where $P = [\max(F_o^2, 0) + 2F_c^2]/3$. The A values are 0.1200, 0.1127, and 0.0565 for **1**–**3**, respectively, with a B value of 0.0 for all of them.

atoms were generated and refined using a riding model with fixed thermal parameters. Among the solvent molecules the oxygen atom O6 of water was located in a special position and refined with a site occupancy factor of 0.5. The other positionally disordered solvent water molecules O5 and O7–O10 were assigned site occupancy factors of 0.7, 0.7, 0.5, 0.3, and 0.3 respectively, with SHELX. All the oxygen atoms of the solvent molecules were refined isotropically and blocked during the last few cycles of refinement to lower the shift/esd value.

Single crystals of complex **3** were obtained by slow concentration of a solution of the complex in a THF/MeOH mixture (1:1, v/v) at room temperature. A crystal of dimensions $0.24\times0.15\times0.10\ mm^3$ was mounted on a glass fiber with epoxy cement and the diffraction data were obtained with a Bruker SMART APEX CCD diffractometer at 293(2) K using a scan speed of 10 s per frame with increasing ω (width of 0.3° per frame). Empirical absorption corrections on the intensity data were made.[39] The structure of **3** was determined in a similar way as described above for **1**. All non-hydrogen atoms of the complex were refined anisotropically. The hydrogen atoms attached to the carbon atoms were located from the difference Fourier map and refined isotropically; they were blocked during the last few cycles of refinement to lower the shift/esd value. The oxygen atoms O5 and O6 of solvent water molecules were located at special positions. Other than the solvent water molecule, there is also half a THF molecule in the asymmetric unit. The goodness-of-fit (GoF) and the maximum shift/esd values were 1.018 and 0.0, respectively. Selected crystallographic data are presented in Table 4. Perspective views of the molecules were produced with ORTEP.[42]

CCDC-214522 (**1**), CCDC-252448 (**2**), and CCDC-252449 (**3**) contain the supplementary crystallographic data for this paper. These data can be obtained free of charge from The Cambridge Crystallographic Data Centre via www.ccdc.cam.ac.uk/data request/cif.

Acknowledgements

We thank the Department of Science and Technology, Government of India, for financial support (grant SP/S1/F-01/2000) and for the CCD facility. We also thank the Convener, Bioinformatics Center of our Institute for the database search.

[1] a) S. J. Lippard, J. M. Berg, *Principles of Bioinorganic Chemistry*, University Science Books, Mill Valley, CA, **1994**. b) W. Kaim, B. Schwerderski, *Bioinorganic Chemistry: Inorganic Elements in the Chemistry of Life*, John Wiley, Chichester, **1994**. c) *Multi-Copper Oxidases* (Ed.: A. Messerschimdt), World Scientific, Singapore, **1997**.

[2] a) R. H. Holm, P. Kennepohl, E. I. Solomon, *Chem. Rev.* **1996**, *96*, 2239–2314; b) E. I. Solomon, M. D. Lowery, *Science* **1993**, *259*, 1575–1580; c) E. I. Solomon, M. J. Baldwin, M. D. Lowery, *Chem. Rev.* **1992**, *92*, 521–542; d) J. A. Fee, *Struct. Bonding (Berlin)* **1975**, *23*, 1–60.

[3] B. Reihammar, *The Coordination Chemistry of Metalloenzymes: The Role of Metals in Reactions Involving Water, Dioxygen and Related Species* (Eds.: I. Bertini, R. S. Drago, C. Luchinat), D. Reidel, Dordrecht, **1982**.

[4] a) S. S. Mukhopadhyay, R. J. Staples, W. W. Armstrong, *Chem. Commun.* **2002**, 864–865; b) S. Gou, M. Qian, Z. Yu, C. Duan, X. Sun, W. Huang, *J. Chem. Soc. Dalton Trans.* **2001**, 3232–3237; c) P. E. Kruger, B. Moubaraki, G. D. Fallon, K. S. Murray, *J. Chem. Soc. Dalton Trans.* **2000**, 713–718; d) S. Yamanaka, H. Okawa, K. Motoda, M. Yonemura, D. E. Fenton, M. Ebadi, A. B. P. lever, *Inorg. Chem.* **1999**, *38*, 1825–1830; e) J. L. Cole, L. Avigliao, L. Morpugno, E. I. Solomon, *J. Am. Chem. Soc.* **1991**, *113*, 9080–9089.

[5] a) D. Gatteschi, R. Sessoli, *Angew. Chem.* **2003**, *115*, 278–309; *Angew. Chem. Int. Ed.* **2003**, *42*, 268–297; b) R. E. P. Winpenny, *Adv. Inorg. Chem.* **2001**, *52*, 1–111; c) K. S. Murray, *Adv. Inorg. Chem.* **1995**, *43*, 261–358.

[6] a) C. Boskovic, E. K. Brechin, W. E. Streib, K. Folting, J. C. Bollinger, D. N. Hendrickson, G. Christou, *J. Am. Chem. Soc.* **2002**, *124*, 3725–3736; b) V. G. Makhankova, O. Y. Vassilyeva, V. N. Kokozay, B. W. Skelton, J. Reedijk, G. A. Vanalbada, L. Sorace, D. Gatteschi, *New J. Chem.* **2001**, *25*, 685–689; c) H. Andres, R. Basler, H.-U. Güdel, G. Aromí, G. Christou, H. Büttner, B. Rufflé, *J. Am. Chem. Soc.* **2000**, *50*, 12469–12477; d) R. Sessoli, H.-L. Tsai, A. R. Schake, S. Wang, J. B. Vincent, K. Folting, D. Gatteschi, G. Christou, D. N. Hendrickson, *J. Am. Chem. Soc.* **1993**, *115*, 1804–1816.

[7] a) L. Chun, C. R. Kagan, *J. Am. Chem. Soc.* **2003**, *125*, 336–337; b) H. E. Toma, *J. Braz. Chem. Soc.* **2003**, *14*, 845–869.

[8] a) A. Bousseksou, G. Molnar, P. Demont, J. Menegotto, *J. Mater. Chem.* **2003**, *13*, 2069–2071; b) E. Coronado, J. R. Galan-Mascaros, C. J. Gomez-Garcia, V. Laukhin, *Nature* **2000**, *408*, 447–449; c) J. S. Miller, *Inorg. Chem.* **2000**, *39*, 4392–4408.

[9] a) *Copper Coordination Chemistry: Biochemical and Inorganic Perspectives* (Eds.: K. D. Karlin, J. Zubieta), Adenine Press, New York, **1983**. b) B. J. Hathaway, *Comprehensive Coordination Chemistry, Vol. 5*, (Eds.: G. Wilkinson, R. D. Gillard, J. A. McCleverty), Pergamon Press, Oxford, **1987**, p. 533; c) O. Kahn, *Angew. Chem.* **1985**, *97*, 837; *Angew. Chem. Int. Ed. Engl.* **1985**, *24*, 834.

[10] a) A. Messerschmidt, *Struct. Bonding (Berlin)* **1998**, *90*, 37–68; b) E. I. Solomon, U. M. Sundaram, T. E. Machonkin, *Chem. Rev.* **1996**, *96*, 2563–2605; c) T. E. Machonkin, E. I. Solomon, *J. Am. Chem. Soc.* **2000**, *122*, 12547–12560.

[11] A. Mukherjee, I. Rudra, S. G. Naik, S. Ramasesha, M. Nethaji, A. R. Chakravarty, *Inorg. Chem.* **2003**, *42*, 5660–5668.

[12] A. Mukherjee, M. K. Saha, I. Rudra, S. Ramasesha, M. Nethaji, A. R. Chakravarty, *Inorg. Chim. Acta* **2004**, *357*, 1077–1082.

[13] A. Mukherjee, I. Rudra, S. Ramasesha, M. Nethaji, A. R. Chakravarty, *Inorg. Chem.* **2003**, *42*, 463–468.

[14] A. Mukherjee, M. Nethaji, A. R. Chakravarty, *Chem. Commun.* **2003**, 2978–2979.

[15] K. Geetha, M. Nethaji, A. R. Chakravarty, *Inorg. Chem.* **1997**, *36*, 6134–6137.

[16] a) L. Merz, W. Haase, *J. Chem. Soc. Dalton Trans.* **1978**, 1594–1598; b) R. Mergehenn, L. Merz, W. Haase, *J. Chem. Soc. Dalton Trans.* **1980**, 1703–1709.

[17] L. Walz, H. Paulus, W. Haase, *J. Chem. Soc. Dalton Trans.* **1983**, 657–666.

[18] H. Astheimer, F. Nepveu, L. Walz, W. Haase, *J. Chem. Soc. Dalton Trans.* **1985**, 315–320.

[19] J. Sletten, A. Sørensen, M. Julve, Y. Journaux, *Inorg. Chem.* **1990**, *29*, 5054–5058.

[20] H. Oshio, Y. Saito, T. Ito, *Angew. Chem.* **1997**, *109*, 2789–2791; *Angew. Chem. Int. Ed. Engl.* **1997**, *36*, 2673–2675.

[21] X. Shi-Tan, R. Nukada, M. Mikuriya, Y. Nakano, *J. Chem. Soc. Dalton Trans.* **1999**, 2415–2416.

[22] R. Wegner, M. Gottschaldt, H. Görls, E.-G. Jäger, D. Klemm, *Chem. Eur. J.* **2001**, *7*, 2143–2157.

[23] A. Mukherjee, M. Nethaji, A. R. Chakravarty, *Angew. Chem.* **2004**, *116*, 89–92; *Angew. Chem. Int. Ed.* **2004**, *43*, 87–90.

[24] L. Schwabe, W. Haase, *J. Chem. Soc. Dalton Trans.* **1985**, 1909–1914.

[25] N. Matsumoto, T. Kondo, M. Kodera, H. Okawa, S. Kida, *Bull. Chem. Soc. Jpn.* **1989**, *62*, 4041–4043.

[26] G. D. Fallon, B. Moubaraki, K. S. Murray, A. M. Van Den Bergen, B. O. West, *Polyhedron* **1993**, *12*, 1989–2000.

[27] S. Wang, J.-C. Zheng, L. K. Thompson, *Polyhedron* **1994**, *13*, 1039–1044.

[28] U. Turpeinen, R. Hamalinen, I. Mutikainen, *Acta. Crystallogr., Sect. C* **1999**, *55*, 50–52.

[29] C. Sirio, O. Poncelet, L. G. Hubert-Pfalzgraf, J. C. Daran, J. Vaissermann, *Polyhedron* **1992**, *11*, 177–184.

[30] J. Sletten, A. Sorensen, M. Julve, Y. Journaux, *Inorg. Chem.* **1990**, *29*, 5054–5058.

[31] E. Gojon, J.-M. Latour, S. J. Greaves, D. C. Povey, V. Ramdas, G. W. Smith, *J. Chem. Soc. Dalton Trans.* **1990**, 2043–2051.

[32] J.-P. Lauret, J.-J. Bonet, F. Nepveu, H. Astheimer, L. Wals, W. Haase, *J. Chem. Soc. Dalton Trans.* **1982**, 2433–2438.
[33] H. Muhonen, *Acta Chem. Scand. A* **1980**, *34*, 79–83.
[34] a) M. Ahlgren, U. Turpeinen, R. Hamalienen *Acta Crystallogr., Sect. B* **1982**, *38*, 429–433; b) L.-P. Wu, T. Kuroda-Sowa, M. Maekawa, Y. Suenaga, M. Munakata, *J. Chem. Soc. Dalton Trans.* **1996**, 2179–2180.
[35] S. K. Pati, S. Ramasesha, D. Sen in *Magnetoscience—From Molecules to Materials (IV)* (Eds.: J. Miller, M. Drillon), Wiley-VCH, Germany, **2003**, 119.
[36] E. R. Davidson, *J. Comp. Physiol.* **1975**, *17*, 87–94.
[37] Y. Nishida, S. Kida, *J. Chem. Soc. Dalton Trans.* **1986**, 2633–2640.
[38] W. Mazurek, B. J. Kennedy, K. S. Murray, M. J. O'Connor, J. R. Rodgers, M. R. Snow, A. G. Wedd, P. R. Zwack, *Inorg. Chem.* **1985**, *24*, 3258–3264.
[39] a) Bruker SMART and SAINT, Version 6.22a, Bruker AXS Inc., Madison, Wisconsin, USA, **1999**; b)G. M. Sheldrick, SADABS, Version 2. Multi-Scan Absorption Correction Program, University of Göttingen, Germany, **2001**.
[40] G. M. Sheldrick, SHELX 97, Programs for Crystal Structure Solution and Refinement, University of Göttingen, Göttingen, Germany, **1997**.
[41] A. C. T. North, D. C. Phillips, F. S. Mathews, *Acta. Crystallogr., Sect. A* **1968**, *24*, 351–359.
[42] M. N. Burnett, C. K. Johnson, *ORTEP-III*, Report ORNL-6895, Oak Ridge National Laboratory, Oak Ridge, TN, **1996**.

Received: October 14, 2004
Published online: March 15, 2005